ChemElectroChem

Research Article
doi.org/10.1002/celc.202500013

Chemistry Europe
European Chemical Societies Publishing

www.chemelectrochem.org

Machine Learning-Assisted Pulse Electrodeposition of Copper for Enhanced Nitrate Sensing

Seyed Oveis Mirabootalebi,[a] Annalise Mackie,[a] Gideon Vos,[a] Mostafa Rahimi Azghadi,[a] and Yang Liu*[a]

Overexposure to nitrate, the most stable and prevalent form of dissolved inorganic nitrogen, harms the environment, causing soil acidification, eutrophication, and water contamination. Among various methods for nitrate detection, electrochemical sensors have attracted considerable attention due to their inherent simplicity, high sensitivity, and low cost. However, several challenges remain, including the overpotential for nitrate reduction reaction, which leads to poor selectivity, repeatability and stability. In this work, copper modified electrodes fabricated by pulse electrodeposition method were developed for the selective detection of nitrate. The electrode modification process that determines the sensing performance was investigated by machine learning approaches to understand the relationship between the sensors' output and the copper deposition parameters. The developed networks successfully predicted the peak current, peak potential, and current stability for electrochemical reduction of nitrate based on the pulse electrodeposition parameters. Furthermore, the most important parameter that influenced the nitrate reduction peak current was revealed by the sensitivity analysis of the designed networks. The experimental results indicate that the proposed sensor achieved a sensitivity of 9.928 μA/mM and a linear range of 0.1 to 20 mM, along with satisfactory recoveries in real sample analysis.

1. Introduction

Dissolved inorganic nitrogen (DIN) compounds, including ammonium (NH_4^+), nitrite (NO_2^-), and nitrate (NO_3^-), represent the main bioavailable forms of nitrogen, exerting a significant impact on aquatic ecosystems by serving as key limiting nutrients for primary production.[1] During biological nitrification, NH_3 is first oxidized to nitrite, followed by the conversion of NO_2^- to NO_3^-.[2] As a result, NO_3^- is the most stable and prevalent form of DIN compound in water. It is a common risk to freshwater resources, as it is a byproduct of fossil fuel combustion and is also commonly found in manure and fertilizers.[3] The World Health Organization (WHO) has established a limit of 50 mg/L for NO_3^- in drinking water,[4] since excessive concentrations of NO_3^- can disrupt biological systems and may lead to several diseases such as blue baby syndrome.[5] Therefore, high-frequency on-site monitoring of NO_3^- levels is essential for protecting the environment and public health. Several methods, including ion-exchange chromatography,[6] high-performance liquid chromatography,[7] fluorescence,[8] and surface-enhanced Raman spectroscopy,,[9] and electrochemistry[10] have been employed for NO_3^- detection. However, these methods require expensive equipment and specialized laboratory expertise, making them unsuitable for field analysis of environmental samples. Although UV-vis spectroscopic sensors have been widely used for in-situ determination of NO_3^-, their susceptibility to turbidity and high cost limit their applications in environmental water monitoring. To address these challenges, electrochemical techniques have attracted considerable interest due to their high sensitivity, low cost, fast response, and ease of operation, making them highly favourable for on-site water quality monitoring.

Although electrochemical techniques have been widely used for NO_3^- detection, many applications in aquatic analysis are still limited by challenges such as low stability and poor selectivity. These issues may arise from several factors, such as the high overpotential required for NO_3^- reduction, adsorption of NO_3^-reduction byproducts at electrode surface, and the lack of resistance to variations in ionic strength and pH of the matrix.[3,11] Electrode modification with copper (Cu) or silver (Ag) is a common approach to developing electrochemical sensors for the determination of NO_3^-.[12] It has been reported that Cu shows higher catalytic activity than Ag for electrochemical reduction of NO_3^-.[12a] In addition, since the significantly higher cost of Ag compared to Cu could pose a challenge for commercialisation of sensing devices, Cu is more favourable in the development of electrochemical NO_3^- sensors, although improvements in sensing performance, including stability, reproducibity, and linear range, are still needed to meet the requirements of practical applications in environmental monitoring.[13] Electrodeposition is one of the most commonly used methods for modification of electrodes with Cu catalysts, while there is a lack of understanding regarding the effect of deposition parameters on sensing performance due to the variety of deposition procedures and the complexity of electro-

[a] S. Oveis Mirabootalebi, A. Mackie, G. Vos, Dr. M. Rahimi Azghadi, Dr. Y. Liu
College of Science and Engineering
James Cook University
Townsville, Queensland 4811, Australia
E-mail: yang.liu11@jcu.edu.au

Supporting information for this article is available on the WWW under https://doi.org/10.1002/celc.202500013

chemical interfaces. The formation of Cu catalysts via electrodeposition is highly dependent on deposition procedure, as well as the chemical and physical properties of the interface between the electrode surface and the electrolyte. For instance, modifying template materials on the electrode surface can significantly alter the morphology of Cu catalysts by influcing the Cu growth mechanism.[14] Consequently, even slight interfacial changes could lead to substantial variations in the size and size distribution of Cu catalysts, ultimately affecting their catalytic properties. Additionally, substrate electrodes such as glassy carbon electrodes (GCEs) and screen-printed electrodes (SPEs) play a significant role in the stability of modified electrodes, which can be attributed to variations in the physical and chemical properties of the electrode surface.[15] The pulse deposition technique offers greater flexibility in controlling the deposition process compared to conventional deposition method, making it well-suited for integration with machine learning approaches to understand the relationship between fabrication parameters and sensing performance.[16]

In this paper, a pulse electrodeposition technique, combined with machine learning methods, was used to modify electrodes with Cu catalysts for the development of electrochemical sensors for NO_3^- detection. There are various methods for Cu deposition, but pulse plating is a versatile technique for modifying carbon substrates with metals and alloys, offering exceptional capability and flexibility to control thickness at the atomic scale by simply adjusting the pulse deposition parameters.[16] It was found that the pulse parameters for Cu deposition have significant impact on the performance of the NO_3^- sensors including sensitivity and selectivity. Furthermore, the effect of substrate materials for deposition of Cu on sensing performance was investigated by developing two machine learning methods based on the prepared data bank, which enabled the accurate prediction of the peak current, the peak potential and the current stability of the Cu modified electrodes for electrocatalytic reduction of NO_3^-, as well as determining the most influential deposition parameters that affect the current responses.

2. Experimental

2.1. Materials and Chemicals

All chemicals were of analytical grade and used as received without additional purification, and all solutions were prepared using ultrapure water with a resistivity of 18.2 MΩ cm (Milli-Q, Merck). Copper nitrate ($Cu(NO_3)_2$), potassium chloride (KCl), potassium nitrate (KNO_3), potassium sulphate (K_2SO_4), potassium nitrite (KNO_2), potassium acetate (CH_3CO_2K), iron chloride ($FeCl_3$), iron chloride tetrahydrate ($FeCl_2.4H_2O$), manganese chloride tetrahydrate ($MnCl_2 \cdot 4H_2O$), nitric acid (HNO_3) and dipicolinic acid ($C_7H_5NO_4$) were purchased from Merck (Australia). Sodium chloride (NaCl) was sourced from ChemSupply (Australia).

For real sample analysis, the tap water and the river water samples were collected from the laboratory at James Cook University and the Ross River in Townsville, Australia, respectively. These samples were then filtered through a 0.45 μm syringe filter and used as the primary test solutions. SPEs consisting of a carbon working electrode, a Ag reference electrode and a carbon counter electrode were purchased from Metrohm. Glassy carbon working electrodes, Ag/AgCl (1 M KCl) reference electrodes and Pt wire counter electrodes were sourced from CH Instruments, Inc.

2.2. Instrumentation and Methods

Electrochemical measurements were performed using a PalmSens4 potentiostat (PalmSens, Netherlands) in a three-electrode cell. The electrodeposition was performed in a Cu bath containing 0.1 M $Cu(NO_3)_2$, 34 mM nitric acid, 14 mM dipicolinic acid, and 0.1 M KCl, where nitric acid maintained an acidic environment, dipicolinic acid acted as the complexing agent, and KCl functioned as the electrolyte to enhance the ionic strength. Each deposition process was controlled by pulse parameters, including on-time (t_{on}), off-time (t_{off}), applied voltage, and the number of cycles. The electrolyte solution for NO_3^- detection was 0.1 M KCl in the neutral medium. The modified electrodes were stored in a dry place at ambient temperature when not in use. Morphological and elemental analyses of the electrodes were performed using scanning electron microscopy (SEM, JXA-iHP200F).

2.3. Machine Learning Models and Procedures

The artificial neural network (ANN) is a subclass of machine learning processes, consisting of interconnected neurons that communicate with each other through weighted signals.[17] Generally, an ANN consists of input, hidden, and output layers. During the training process, the weights, which determine the strength of the connections between neurons, are adjusted to optimize performance.[18] The output of a neuron in a neural network is given by Eq. (1):

$$x = \sum_{i=1}^{p} w_i x + b \tag{1}$$

Here, x is the neuron's output, p is the number of input connections; w_i represents the weight associated with the i^{th} input; and b is a bias term.

In this work, four important parameters in pulse electrodeposition, including voltage, t_{on} t_{off} , and the number of cycles, are used as inputs. The outputs are the NO_3^- reduction peak current, peak potential, as well as the number of measurements performed on each sensor and their current responses, which indicate the sensor stability. A total of one hundred Cu modified electrodes were fabricated under various deposition parameters, with fifty using SPEs and another fifty using GCEs as substrate electrodes. The inputs and outputs obtained from the Cu/SPEs and the Cu/GCEs were used to design the ANN. In addition, the original Cu/SPE and Cu/GCE datasets were expanded by transforming experiments 1 to 5 for each sensor parameter set through a row-wise pivoting process, resulting in a total of 168 samples per sensor. The expanded datasets were subsequently used as training data for various regression machine learning models, including XGBoost and an ANN.

Initial experiments for the Cu/SPEs using the XGBoost model to predict reduction peak current, following hyperparameter tuning, resulted in a relatively high mean absolute error (MAE) of 16.40. Consequently, focus shifted toward the ANN model. Several activation functions, including ReLU, LeakyReLU and SELU, were evaluated to optimize model performance. The ANN trained with ReLU and SELU activation functions on the Cu/SPEs data achieved significantly lower MAEs compared to XGBoost of 11.80 and 9.65,

respectively. Training employed mean squared error (MSE) as the loss function and the AdamW optimizer, configured with a learning rate of 0.08 and a weight decay of 1×10^{-4}. These hyperparameters were selected through iterative trial runs to determine optimal settings. Training was capped at 1000 epochs, with early stopping implemented using a patience threshold of 5 to mitigate overfitting. Merging of both datasets to form a single larger dataset resulted in significantly higher error rates, indicative of the difference between the Cu/SPEs and the Cu/GCEs.

Given the better performance of the SELU activation function on the Cu/SPE dataset, a custom SELU implementation was explored. The standard scaling factor parameter for SELU was reduced from 1.0507 to 0.8507, which resulted in a further improved MAE for reduction peak current of 8.82, peak potential of 0.01 and 0.19 for the sensor stability. For the Cu/GCEs dataset, a customized LeakyReLU activation function with negative slope parameter reduced to −0.1 from the default 0.01, outperformed ReLU, SELU and the customized SELU functions, producing an MAE of 8.97 for reduction peak current, 0.02 for peak current and 0.43 for sensing stability. This enhancement, through the use of customized activation functions, underscores their critical role in determining ANN performance, and further highlights the fact that default activation function parameters may not yield optimal outcomes, with additional parameter tuning likely to deliver improved modelling results.

3. Results and Discussion

3.1. Voltammetric Behaviour of Cu/SPEs

Cyclic voltammetry (CV) was used to investigate the voltammetric behaviour of NO_3^- at different electrodes. Figure 1 demonstrates the CVs of the bare SPE and the Cu/SPE in the presence of 1 mM NO_3^-. After modification of Cu, the electrode showed two oxidation peaks at −0.6 and −0.4 V, which can be attributed to the oxidation of Cu (I) and Cu (II), respectively. In addition, four reduction peaks (R_1–R_4) observed at −0.25, −0.65, −0.92 and −1.11 V can be associated with the reactions as below:

$$R_1: \ Cu\ (I) + e^- \rightarrow Cu \quad (2)$$

$$R_2: \ Cu\ (II) + 2e^- \rightarrow Cu \quad (3)$$

$$R_3: \ NO_3^- + H_2O + 2e^- \rightarrow NO_2^- + 2OH^- \quad (4)$$

$$R_4: \ NO_2^- + 5H_2O + 2e^- \rightarrow NH_3 + 7OH^- \quad (5)$$

Although the peaks associated with R_1, R_2, and R_4 were indirectly affected by the NO_3^-concentrations, the simultaneous reduction of Cu ions and the catalytic effect of cupric ions on nitrogen-based compounds may result in low accuracy for NO_3^- sensing.[13a,19] Therefore, the peak of R_3 observed at −0.92 V for the reduction of NO_3^- to NO_2^- was used for all measurements in this work.

To investigate the electrochemical process of NO_3^- reduction at the Cu/SPEs, CV was performed at scan rates ranging from 0.1 to 0.5 V/s (Figure 2A). The results indicate that the reduction peak current of NO_3^- increases linearly with the square root of scan rate, suggesting that the electrochemical process is diffusion-controlled, as shown in Figure 2B.[20]

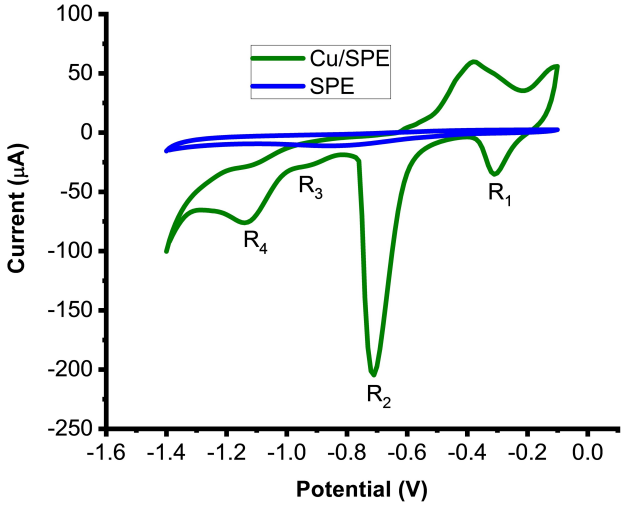

Figure 1. CVs of the bare SPE (blue curve) and the Cu/SPE (green curve) in 0.1 M KCl containing 1 mM NO_3^- at scan rate of 0.1 V/s.

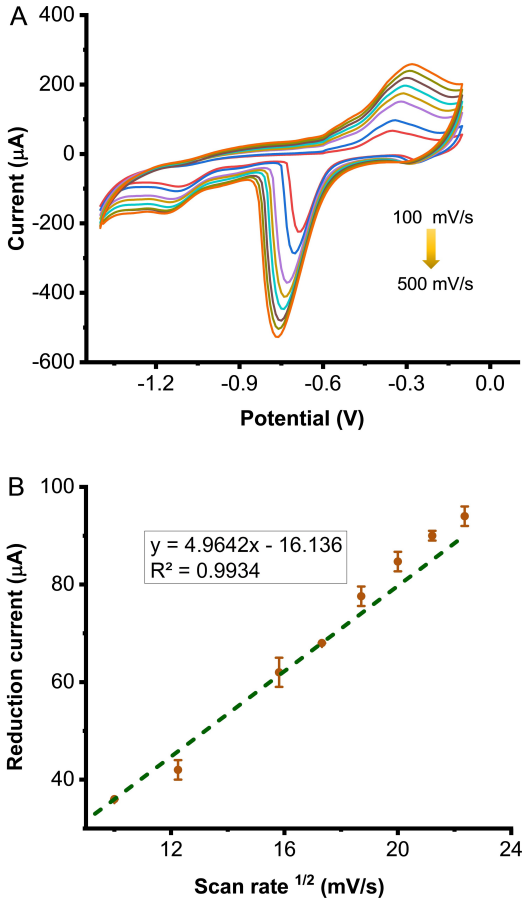

Figure 2. (A) CVs of 1 mM NO_3^- at the Cu/SPE with different scan rates (100, 150, 250, 300, 350, 400, 450, and 500 mV/s). Electrolyte solution: 0.1 M KCl. (B) Linear relationship of the NO_3^- reduction peak current versus square root of scan rate.

3.2. Effect of Pulse Parameters on NO_3^- Sensing

Compared to continuous electrodeposition, the pulse deposition can provide enhanced mass transfer of metal ions[21] and improved properties of the deposited materials including surface uniformity,[22] particle density[23] and electrical conductivity.[24] These can be attributed to the adjustable parameters of this technique, such as t_{off}, which may affect the nucleation and growth of the Cu clusters, and thus accurately control the morphology of the deposited Cu.[14b] Herein, four parameters in pulse electrodeposition method including deposition potential, number of cycles, t_{on}, and t_{off}[25] were evaluated to investigate their effect on the electrochemical reduction of NO_3^- to NO_2^- at the Cu modified electrodes. Linear sweep voltammetry (LSV) was used to measure the peaks of NO_3^-reduction reaction. Figure 3A shows the LSV curves of 1 mM NO_3^- at the Cu/SPEs prepared under different deposition conditions: (a) $E_{dc} = -0.9$ V, $t_{on} = t_{off} = 0.5$ s, $t_{deposition} = 93$ s; (b) $E_{dc} = -0.7$ V, $t_{on} = 0.5$ s, $t_{off} = 1.5$ s, $t_{deposition} = 130.5$ s, indicating that the pulse parameters have a significant effect on the current response to NO_3^-. The microstructures of these Cu/SPEs are depicted in Figure 3B and 3 C, highlighting remarkable differences in the Cu particle size and density on the electrode surface, which can be attributed to the variations in the deposition conditions. This was further confirmed by the Energy Dispersive X-ray (EDX) results of the Cu/SPEs prepared under different conditions (Figure S1 and S2).

It was reported that the electrocatalytic activity of deposited Cu is highly influenced by its morphology, which is governed by the electrodeposition parameters. For instance, uniform coverage of fine Cu clusters is a key to achieving the synergetic effects of the catalysts.[12b,26] Herein, the Cu/SPE prepared under condition b exhibits a more homogeneous distribution of smaller Cu particles compared to condition a, resuting in a higher current response for NO_3^- reduction, which is promising for the development of NO_3^- sensors with higher sensitivity. Although the pulse deposition method offers enhanced controllability by introducing a greater number of adjustable variables, it substantially increases the complexity of identifying the influence of the parameters on sensing performance. Therefore, a machine learning modelling approach was employed to optimize the deposition parameters and understand their impact on the electroanlaytical properties of the deposited Cu catalysts.

The sensing performance of the Cu modified electrodes was evaluated by the four outputs including the NO_3^- reduction peak current and peak potential, as well as the number of measurements performed on each sensor and their current responses, which reflect the stability and reusability of a sensor. To evaluate the network's performance in predicting the outputs, 10% of the experimental data obtained at both Cu/SPEs and Cu/GCEs were used. The validation results of the network show a close agreement between the designed network outcomes and actual values, demonstrating the homogeneity of the experimental and regenerated datasets (Supporting Information, Table S1). This confirms that maintaining consistent Cu deposition conditions leads to repeatable and predictable sensing performance of the Cu modified electrodes.[27] Furthermore, it indicates that the properties of the Cu catalysts formed in a pulse deposition process is predictable, which was in good agreement with the previous studies.[28]

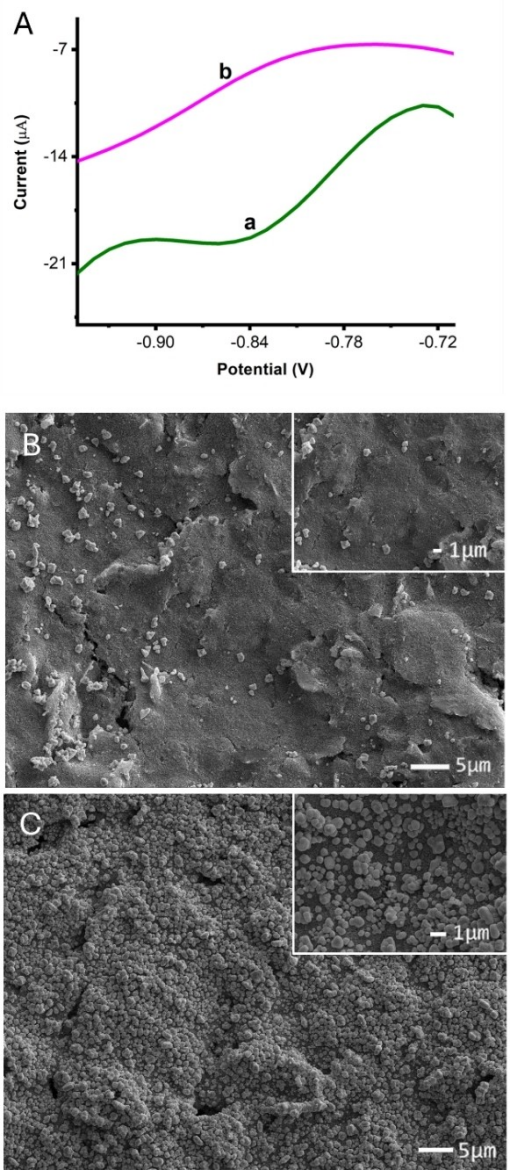

Figure 3. (A) LSV comparison of 1 mM NO_3^- at the Cu/SPEs prepared under the conditions of $E_{dc} = -0.9$ V, $t_{on} = t_{off} = 0.5$ s, $t_{deposition} = 93$ s (a) and $E_{dc} = -0.7$ V, $t_{on} = 0.5$ s, $t_{off} = 1.5$ s, $t_{deposition} = 130.5$ s (b). (B) SEM images of the Cu/SPE prepared to run curve a in A. Inset shows the magnified image. (C) SEM images of the Cu/SPE prepared to run curve b in A. Inset shows the magnified image.

Figure 4 illustrates the modelling results regarding the effect of different pulse deposition parameters on the NO_3^- reduction peak current at the Cu/SPEs and the Cu/GCEs. It was found that t_{off} acts as the most important parameter for the current response towards NO_3^- reduction at both modified electrodes, suggesting that the period during which no potential was applied played a significant role in the nucleation

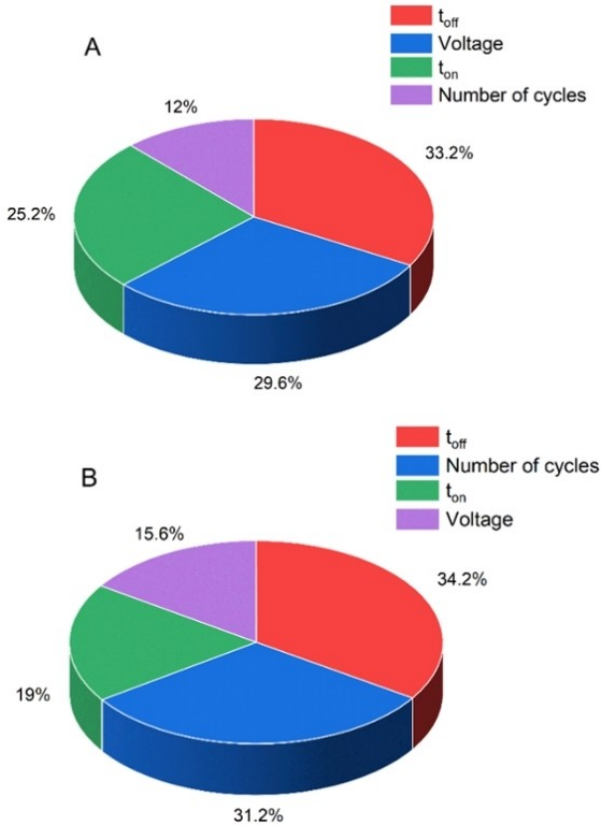

Figure 4. The effect of different pulse deposition parameters on the NO_3^- reduction peak current at the Cu/SPEs (A) and the Cu/GCEs (B).

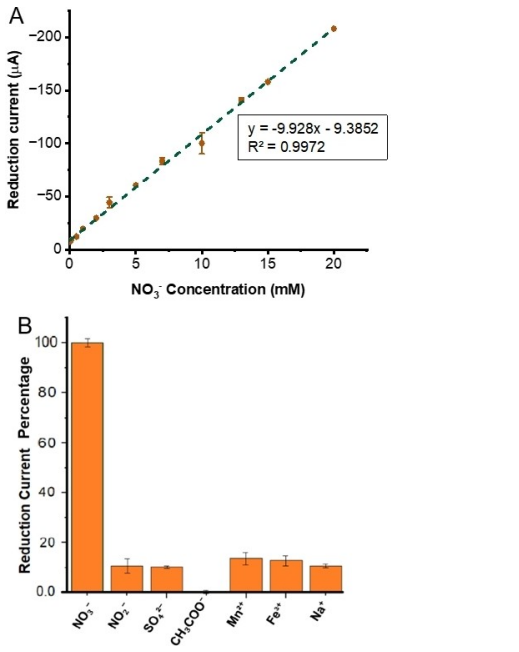

Figure 5. (A) Calibration curve of the Cu/SPEs for detection of NO_3^- in 0.1 M KCl. (B) Selectivity test of the Cu/SPEs (concentration of NO_3^- and interfering ions: 1 mM).

and growth of Cu catalysts.[29] Notably, the pulse deposition parameters exhibited different effects of on the sensing performance of Cu/SPEs and Cu/GCEs. For instance, the deposition voltage is an important factor influencing the peak current obtained at Cu/SPEs, while it has minimal impact on Cu/GCEs. In addition, the number of cycles for Cu deposition plays a significant role in the NO_3^- reduction current obtained at the Cu/GCEs, while it has little effect on Cu/SPEs. This may be attributed to the distinct surface properties of SPEs and GCEs, including differences in roughness, porosity, size, and composition, which may influence the mass transport of Cu ions during the electrodeposition process, and consequently, their performance for NO_3^- detection. However, the underlying reasons are still under investigation.

3.3. Sensing Performance of Cu/SPEs

The performance of the Cu/SPEs prepared under the optimised conditions for NO_3^- sensing was investigated. Figure 5A presents the calibration curve for the detection of NO_3^-, plotted based on its reduction peaks in Figure S3. The curve demonstrates a wide linear range of 0.1 to 20 mM and a high sensitivity of 9.928 μA/mM, which are superior to those obtained with many electrochemical NO_3^- sensors reported previously (Table 1). Another attractive feature of the proposed sensor is its ability to perform measurements in neutral

Table 1. Comparison of the analytical performance of electrochemical sensors for NO_3^- detection.

Electrode	pH	Linear range (mM)	Sensitivity	Reference
Boron-doped diamond film	1.5	0.005–0.214	0.25 μA/mM	[13b]
Arrays of Cu nanowire	3.0	0.01–0.4	50 μA/mM	[14a]
Cu modified silver SPE	neutral	0.05–5	19.08 μA/mM	[13a]
Nanowire-based Cu electrode	2	0.008–5.860	1.375 mA/mM	[30]
Cadmium sulfide nanorods modified SPE	neutral	0.05–5	–	[31]
Cu nanoparticles-polyaniline nanocomposite	5	0.001 - 100	0.15 and 0.88 μA/mM	[32]
Carbon fibres microelectrodes	2	0.005–8	–	[11c]
Gold nanoparticles carbon SPE	7	0.00001–0.004	0.85 $\mu A \cdot \mu M^{-1} \cdot cm^{-2}$	[33]
Cu modified carbon SPE	neutral	0.1–20	9.928 μA/mM	This work

solutions under atmospheric conditions, making it convenient for practical applications.

Interference study was conducted to evaluate the selectivity of the Cu/SPEs for NO_3^- analysis. Considering the environmental water matrix, 1 mM Na^+, Mn^{2+}, CH_3COO^-, NO_2^-, SO_4^{2-}, and Fe^{3+} were selected to investigate their interference effect on the current response of 1 mM NO_3^-. As illustrated in Figure 5B, the percentage of the current response for the interferents relative to that of the analyte was less than 15%, indicating that the proposed sensor exhibits acceptable selectivity for applications in detecting NO_3^- in environmental water samples.

To evaluate the reproducibility of the Cu/SPEs for NO_3^- detection, the current responses of Cu/SPE electrodes to NO_3^- across five different concentrations were tested (Figure 6A). The results show that the relative standard deviations (RSDs) were less than 3.12%, demonstrating satisfactory performance for practical applications. Repeatability test was performed by recording the current response of a Cu/SPE to 1 mM NO_3^- over eight consecutive measurements. As shown in Figure 6B, the current of NO_3^- at the proposed sensor remains at 81% of the initial value after eight uses, although exfoliation of the Cu catalysts may occur during extended measurements. In addition, the long-term stability of the Cu/SPEs were examined by measuring the reduction current of 1 mM NO_3^- at a Cu/SPE every five days. Figure 6C indicates that the signal of the proposed sensor remained stable over 20 days, making it a promising candidate for practical applications.

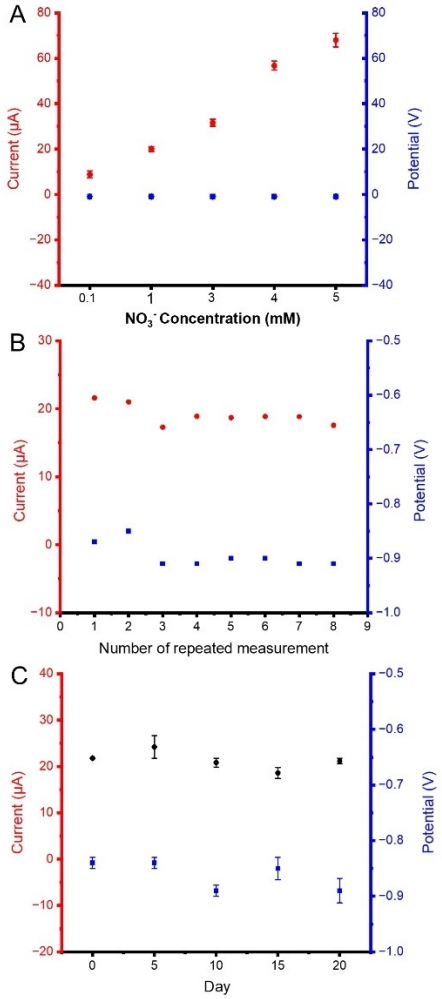

Figure 6. (A) Reproducibility test of Cu/SPEs for detection of NO_3^- at concentrations of 0.1, 1, 2, 5, and 7 mM. (B) Repeatability test of 1 mM NO_3^- at the Cu/SPEs. (C) Stability test of 1 mM NO_3^- at the Cu/SPEs conducted every

Real sample analysis of tap and river waters was conducted to evaluate the applicability of the proposed Cu/SPEs for NO_3^- sensing. The standard addition method was employed by spiking 1 mM NO_3^- into the real samples to assess the matrix effect. The results shown in Table 2 demonstrate the satisfactory recoveries of the Cu/SPEs for detection of NO_3^- in real water samples. In addition, the measurements were carried out in neutral solutions without any sample pre-treatment procedures, which is advantageous over many electrochemical NO_3^- sensors reported previously, as they usually require conducting tests in acidic electrolyte to facilitate the NO_3^- reduction process.[34] Although nanostructured materials have been developed to address this issue, the manufacturing of electrode materials, along with their reproducibility and stability, may limit their use in developing cost-effective and high-performance sensors in environmental applications.[14a,35]

4. Conclusions

In this work, a pulse electrodeposition technique combined with a machine learning method was developed to prepare Cu modified electrodes for NO_3^- detection. As the Cu catalysts formed under different pulse deposition parameters and on different substrate electrodes exhibited distinct electrochemical activities towards NO_3^- reduction, machine learning approaches were designed to investigate the effect of deposition voltage, on-time, off-time and number of deposition cycles on the voltametric behaviour of NO_3^- at both Cu/SPEs and Cu/GCEs. This strategy enables understanding the relationship between sensor fabrication procedures and sensing performance without the need for numerous laboratory tests and resource-intensive efforts. Attractive analytical performance including high sensitivity, wide linear range, good selectivity, and long-term stability was obtained for the determination of NO_3^- at the Cu/SPEs prepared under the optimal conditions. In addition, the proposed sensor was employed for the analysis of NO_3^- in tap and river water samples, showing satisfactory recoveries. This strategy provides a simple and straightforward approach to the design of electrochemical sensors by combining experimental and machine learning methods, paving the way for improving

Table 2. Determination of NO_3^- at the Cu/SPEs in real water samples.

Sample	Added (mM)	Detected (mM)	RSD (%)	Recovery (%)
Tap water	1	1.0161	3.21	101.61
River water	1	1.0280	1.47	102.80

sensor performance and efficiency in a wide range of analytical applications.

Acknowledgements

The authors acknowledge financial support from the James Cook University Postgraduate Research Scholarship and the Australian Academy of Science EMCR Mobility Grant. Open Access publishing facilitated by James Cook University, as part of the Wiley - James Cook University agreement via the Council of Australian University Librarians.

Conflict of Interests

The authors declare no conflict of interest.

Data Availability Statement

The data that support the findings of this study are available from the corresponding author upon reasonable request.

Keywords: Nitrate Detection · Voltammetric Method · Pulse Electrodeposition · Machine Learning · Artificial Neural Network

[1] Y. Wen, W. Zhang, B. Shan, J. Qu, *Journal of Environmental Sciences* **2022**, *122*, 105–114.
[2] T. He, D. Xie, J. Ni, Z. Li, Z. Li, *J. Hazard. Mater.* **2020**, *388*, 122114.
[3] M. P. Mahmud, F. Ejeian, S. Azadi, M. Myers, B. Pejcic, R. Abbassi, A. Razmjou, M. Asadnia, *Chemosphere* **2020**, *259*, 127492.
[4] a) M. Qasemi, M. Darvishian, H. Nadimi, M. Gholamzadeh, M. Afsharnia, M. Farhang, M. Allahdadi, M. Darvishian, A. Zarei, *J. Food Compos. Anal.* **2023**, *115*, 104870; b) C. Jiang, Y. He, Y. Liu, *Analyst* **2020**, *145*, 5400–5413.
[5] M. Choudhary, M. Muduli, S. Ray, *Sustainable Water Resources Management* **2022**, *8*, 113.
[6] P. N. Nesterenko, in *Liquid Chromatography*, Elsevier, **2023**, pp. 465–507.
[7] C. Monton, J. Suksaeree, C. Luprasong, *Scientifica* **2020**, *2020*, 6424682.
[8] R. T. Masserini Jr, K. A. Fanning, *Mar. Chem.* **2000**, *68*, 323–333.
[9] S. Gajaraj, C. Fan, M. Lin, Z. Hu, *Environ. Monit. Assess.* **2013**, *185*, 5673–5681.
[10] M. Talbi, A. Anurag, C. Tegenkamp, M. B. Ali, O. Kanoun, *Measurement* **2024**, *238*, 115395.
[11] a) A. Adiraju, A. Jalasutram, J. Wang, C. Tegenkamp, O. Kanoun, *Adv. Mater. Interfaces* **2024**, 2400102; b) A. Anurag, A. Al-Hamry, Y. Attuluri, S. Palaniyappan, G. Wagner, D. Dentel, C. Tegenkamp, O. Kanoun, *ChemElectroChem* **2023**, *10*, e202200945; c) G. Li, H. Yuan, J. Mou, E. Dai, H. Zhang, Z. Li, Y. Zhao, Y. Dai, X. Zhang, *Composites Communications* **2022**, *29*, 101043; d) N. Junlapak, A. Numnuam, N. Nontipichet, T. Kangkamano, P. Thavarungkul, P. Kanatharana, S. Khumngern, *ChemNanoMat* **2024**, e202300600.
[12] a) G. Dima, A. De Vooys, M. Koper, *J. Electroanal. Chem.* **2003**, *554*, 15–23; b) H. R. L. Z. Zhad, R. Y. Lai, *Anal. Chim. Acta* **2015**, *892*, 153–159.
[13] a) A. S. Inam, M. A. Costa Angeli, B. Shkodra, A. Douaki, E. Avancini, L. Magagnin, L. Petti, P. Lugli, *ACS Omega* **2021**, *6*, 33523–33532; b) S. Wei, D. Xiao, Y. Li, C. Bian, *Micromachines* **2024**, *15*, 487.
[14] a) A. M. Stortini, L. M. Moretto, A. Mardegan, M. Ongaro, P. Ugo, *Sens. Actuators B* **2015**, *207*, 186–192; b) Y. Li, J. Sun, C. Bian, J. Tong, H. Dong, H. Zhang, S. Xia, *AIP Adv.* **2015**, *5*; c) A. S. Inam, M. A. C. Angeli, B. Shkodra, A. Douaki, E. Avancini, L. Magagnin, L. Petti, P. Lugli, *IEEE Sens. J.* **2022**, *23*, 23966–23974.
[15] a) I. G. Casella, M. Contursi, *J. Solid State Electrochem.* **2012**, *16*, 3739–3746; b) Y. Liu, G. Sun, C. Jiang, X. T. Zheng, L. Zheng, C. M. Li, *Microchim. Acta* **2014**, *181*, 63–70.
[16] a) E. Mariani, W. Giurlani, M. Verrucchi, V. Dell'Aquila, P. L. Nostro, M. Innocenti, *J. Electrochem. Soc.* **2024**, *171*, 012504; b) F. Yoosefan, A. Ashrafi, S. M. onir Vaghefi, *Met. Mater. Int.* **2021**, *27*, 106–117.
[17] S. O. Mirabootalebi, G. H. A. Fakhrabadi, R. Mirahmadi, *Organomet. Chem.* **2021**, *1*, 76–85.
[18] R. Babaheydari, S. O. Mirabootalebi, G. Akbari, H. Salehifar, *Int. J. Eng.* **2023**, *36*, 1932–1941.
[19] E. Filimonov, A. Shcherbakov, *Prot. Met.* **2004**, *40*, 280–285.
[20] O. González-Meza, E. Larios-Durán, A. Gutiérrez-Becerra, N. Casillas, J. Escalante, M. Bárcena-Soto, *J. Solid State Electrochem.* **2019**, *23*, 3123–3133.
[21] W. Tsai, C. Wan, Y. Wang, *J. Appl. Electrochem.* **2002**, *32*, 1371–1378.
[22] W. Hansal, M. Halmdienst, S. Hansal, I. Boussaboua, A. Darchen, *Transactions of the IMF* **2008**, *86*, 115–121.
[23] V. Zarembo, D. Zarembo, in *AIP Conference Proceedings, Vol. 2456*, AIP Publishing, **2022**.
[24] a) Y. Zhao, N. Ye, H. Zhuo, C. Wei, W. Zhou, J. Mao, J. Tang, *Materials* **2021**, *14*, 1233; b) G. Baiocco, S. Genna, E. Menna, N. Ucciardello, *Materials* **2023**, *16*, 854.
[25] A. Balasubramanian, D. Srikumar, G. Raja, G. Saravanan, S. Mohan, *Surf. Eng.* **2009**, *25*, 389–392.
[26] R. Farina, G. D'Arrigo, A. Alberti, S. Scalese, G. E. Capuano, D. Corso, G. A. Screpis, M. A. Coniglio, G. G. Condorelli, S. Libertino, *Sensors* **2024**, *24*, 4501.
[27] K. Hili, D. Fan, V. A. Guzenko, Y. Ekinci, *Microelectron. Eng.* **2015**, *141*, 122–128.
[28] a) R. A. Koochaksaraie, F. Barazandeh, M. Akbari, *Metals* **2022**, *13*, 37; b) Z. Shojaei, G. R. Khayati, *J. Appl. Electrochem.* **2023**, *53*, 1433–1447.
[29] S. Esmailzadeh, T. Shahrabi, Y. Yaghoubinezhad, G. B. Darband, *J. Electroanal. Chem.* **2021**, *881*, 114949.
[30] J. Liang, Y. Zheng, Z. Liu, *Sens. Actuators B* **2016**, *232*, 336–344.
[31] S. Chen, J. Chen, M. Qian, J. Liu, Y. Fang, *Electrochim. Acta* **2023**, *446*, 142077.
[32] H. Essousi, H. Barhoumi, M. Bibani, N. Ktari, F. Wendler, A. Al-Hamry, O. Kanoun, *Journal of Sensors* **2019**, *2019*, 4257125.
[33] M. Talbi, A. Al-Hamry, P. R. Teixeira, L. G. Paterno, M. B. Ali, O. Kanoun, *Chemosensors* **2022**, *10*, 40.
[34] a) E. Pérez-Gallent, M. C. Figueiredo, I. Katsounaros, M. T. Koper, *Electrochim. Acta* **2017**, *227*, 77–84; b) B. Patella, R. Russo, A. O'Riordan, G. Aiello, C. Sunseri, R. Inguanta, *Talanta* **2021**, *221*, 121643.
[35] R. G. Hjort, R. R. Soares, J. Li, D. Jing, L. Hartfiel, B. Chen, B. Van Belle, M. Soupir, E. Smith, E. McLamore, *Microchim. Acta* **2022**, *189*, 122.

Manuscript received: January 16, 2025
Revised manuscript received: February 25, 2025
Version of record online: March 17, 2025